Electronic Supplementary Information (ESI)

Controlled synthesis of V_2O_5/MWCNTs core/shell hybrid aerogels through a mixed growth and self–assembly methodology for supercapacitors with high capacitance and ultralong cycle life

Yingjie Wu, Guohua Gao,* Huiyu Yang, Wenchao Bi, Xin Liang, Yuerou Zhang, Guyu Zhang, and Guangming Wu*

Shanghai Key Laboratory of Special Artificial Microstructure, School of Physics Science and Engineering, Tongji University, Shanghai, 200092, China

E–mail: gao@tongji.edu.cn; wugm@tongji.edu.cn

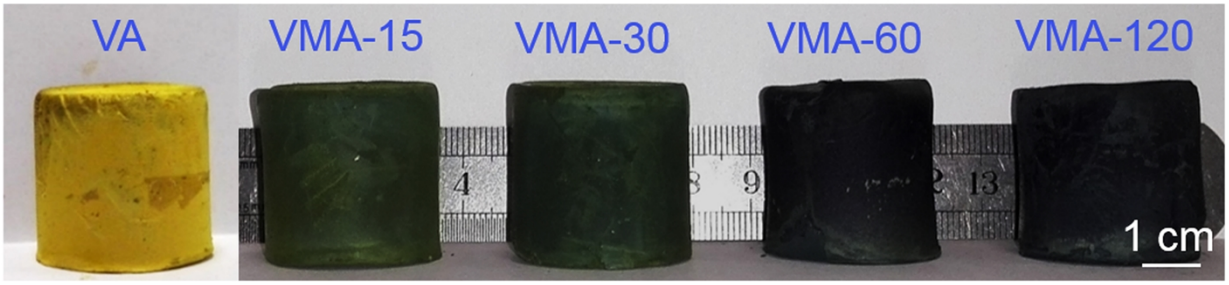

Fig. S1 Digital photographs of as–prepared aerogels.

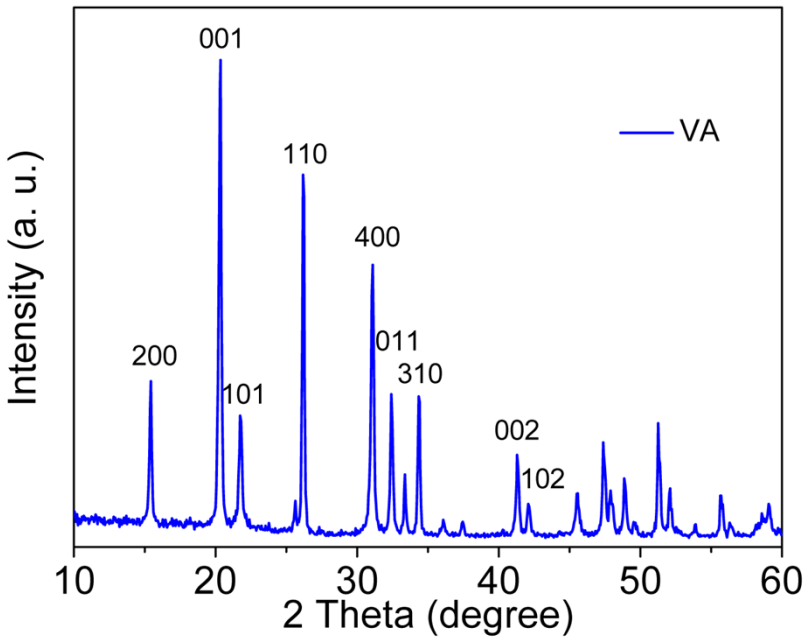

Fig. S2 XRD patterns of crystallized V_2O_5 aerogel after thermal treatment at 300 °C for 3h.

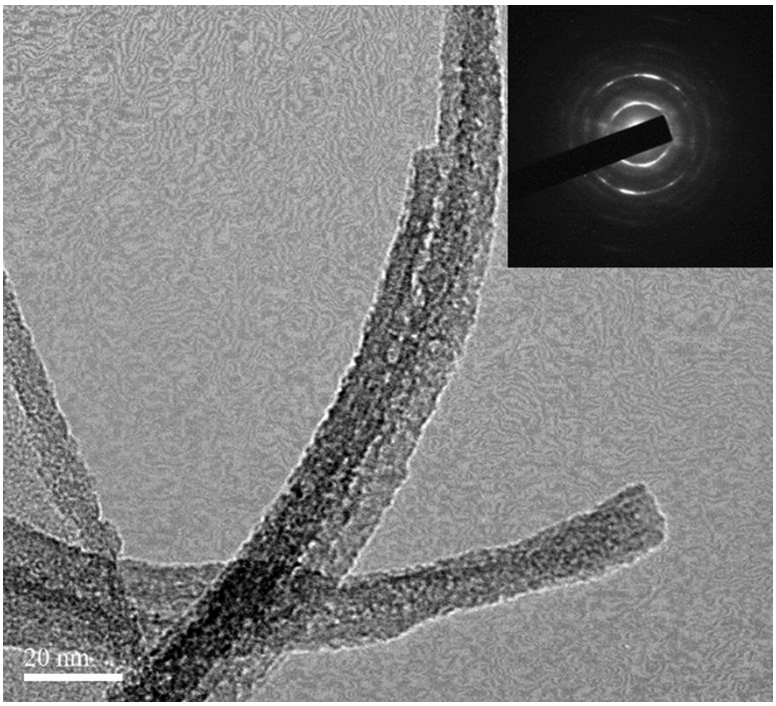

Fig. S3 HRTEM image and SAED patterns (inset) of VO_x nanofibers before thermal treatment.

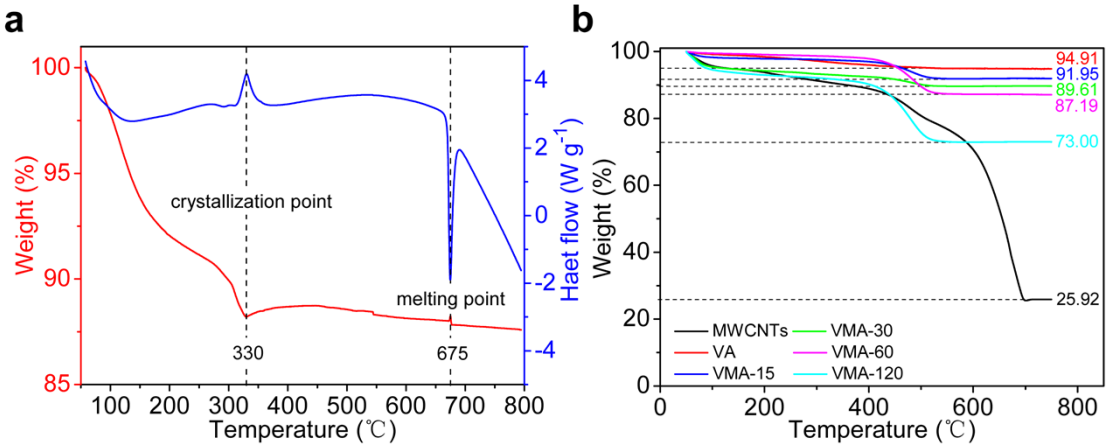

Fig. S4 (a) TG and DSC curves of VO_x aerogel before thermal treatment in air atmosphere, indicating a crystallization point of 330 °C; (b) TG curves of MWCNTs, V_2O_5 aerogel, VMA–15, VMA–30 ,VMA–60 and VMA–120 hybrid aerogels in air.

The content of MWCNTs (C_M) in hybrid aerogels is calculated according to their TG curves by using the formula $W = 0.9491(1 - C_M) + 0.2592C_M$, where W stands for the final weight of hybrid aerogels in TG curves, 0.9491 and 0.2592 is the final weight of pure V_2O_5 aerogel and pure MWCNTs, respectively.

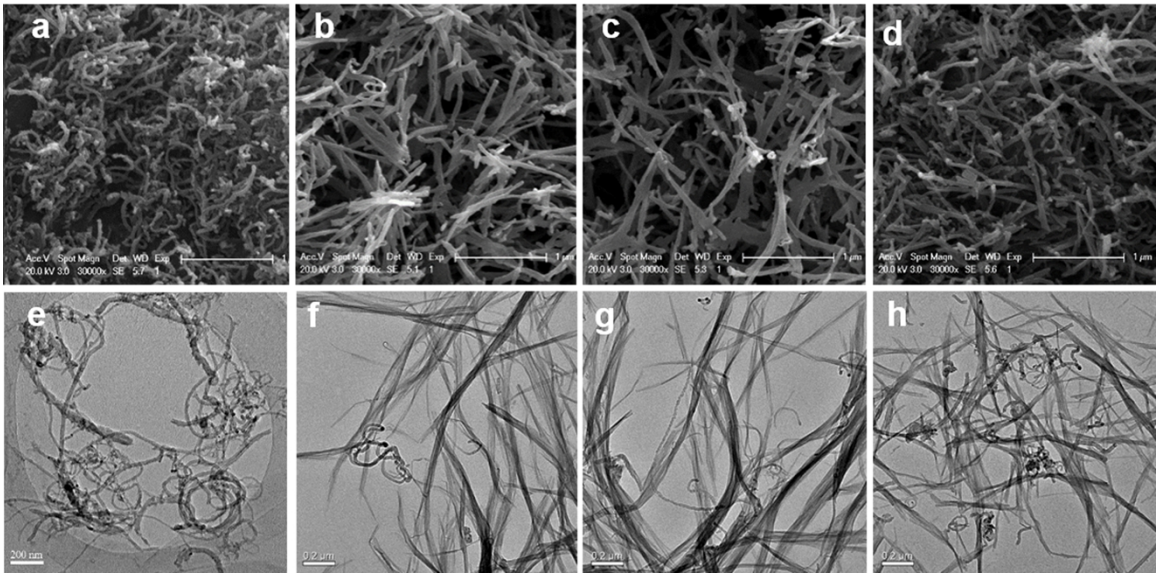

Fig. S5 SEM and TEM images of (a, e) MWCNTs, (b, f) VMA–15, (c, g) VMA–30 and (d, h) VMA–60, respectively.

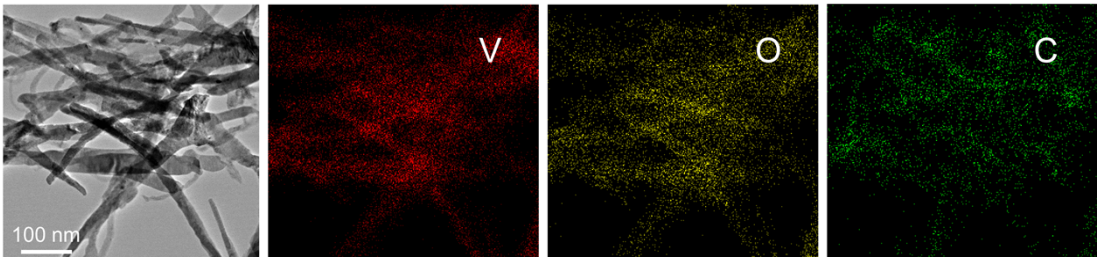

Fig. S6 STEM images and corresponding elemental mapping of V_2O_5/MWCNTs core/shell hybrid aerogels.

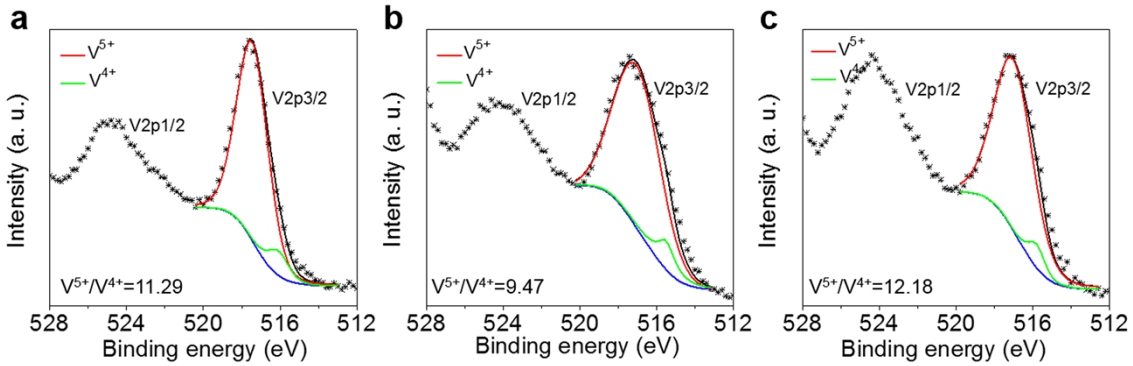

Fig. S7 XPS spectra of V2p3/2 in (a) VMA–15, (b) VMA–30 and (c) VMA–60.

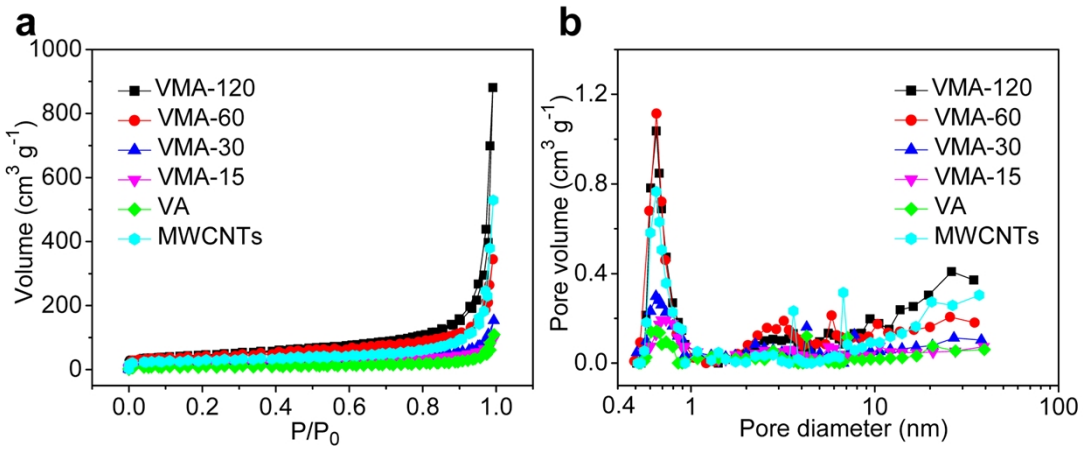

Fig. S8 Nitrogen adsorption–desorption isotherms (a) and Barrett–Joyner–Halenda (BJH) pore–size distribution (b) of acid–treated MWCNTs, prepared V_2O_5 aerogel and V_2O_5/MWCNTs core/shell hybrid aerogels.

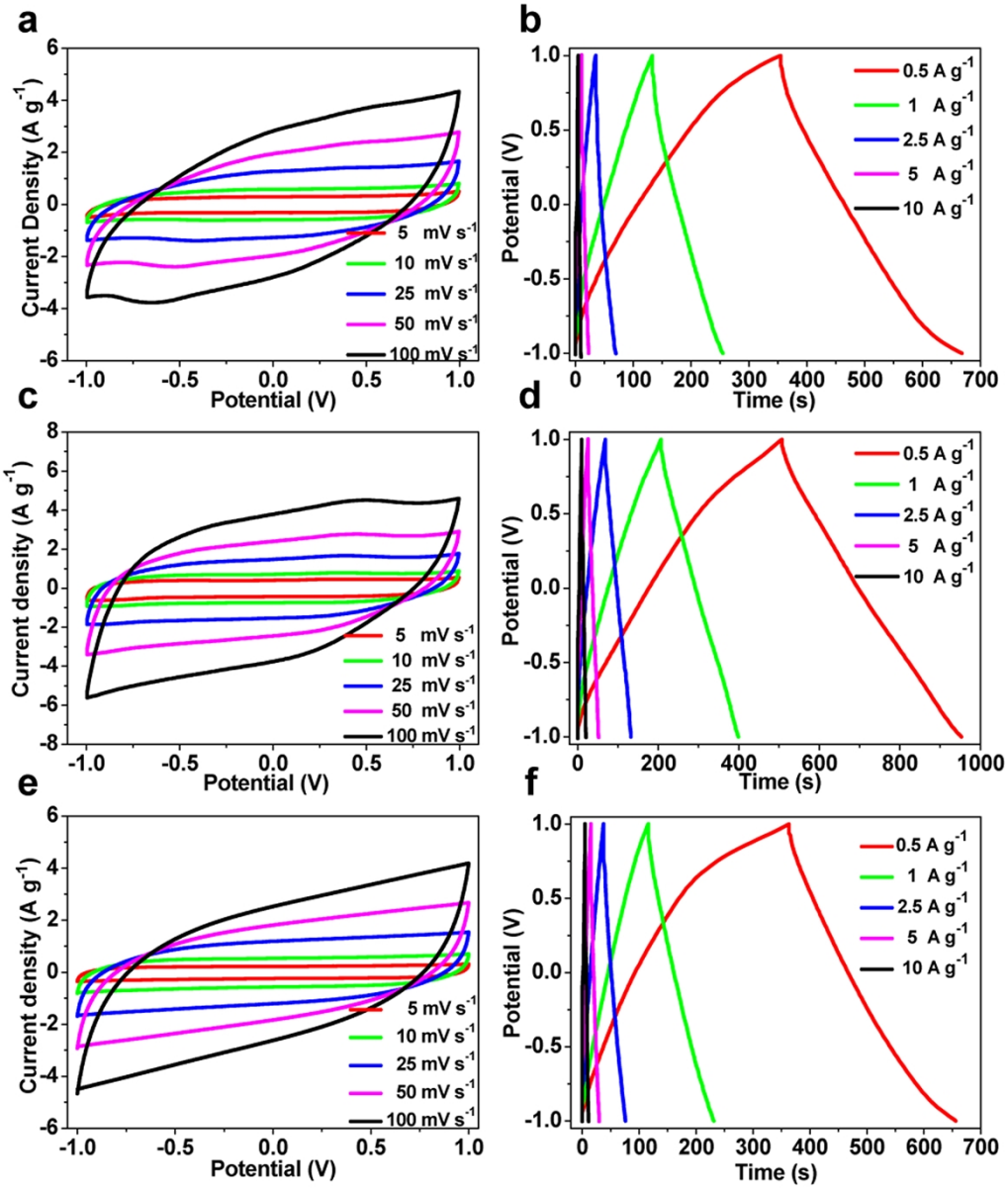

Fig. S9 CV and galvanostatic charge/discharge curves of (a, b) raw V_2O_5 powder, (c, d) original V_2O_5 aerogel and (e, f) MWCNTs, respectively.

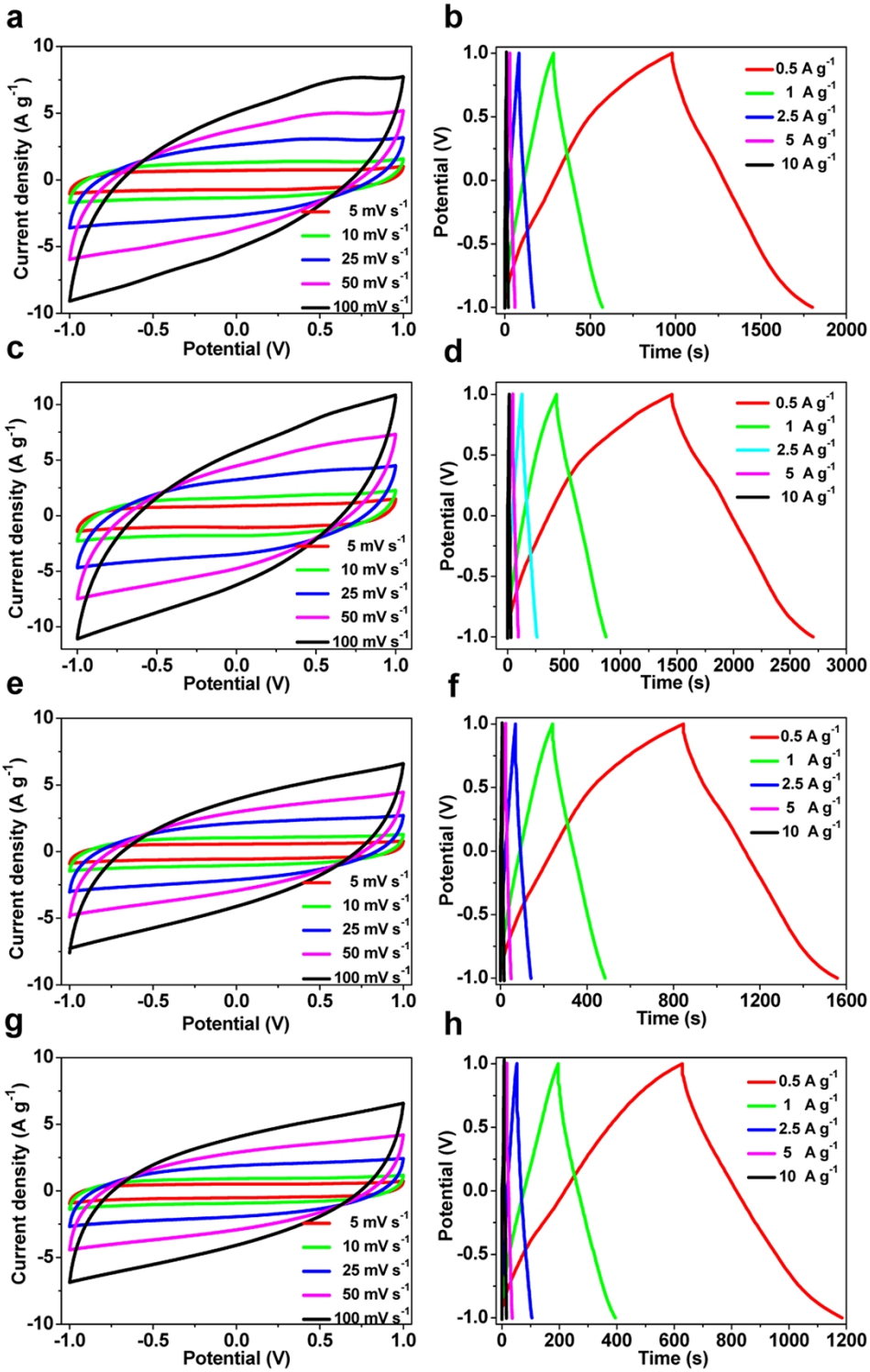

Fig. S10 CV and galvanostatic charge/discharge curves of (a, b) VMA–15, (c, d) VMA–30, (e, f) VMA–60 and (g, h) VMA–120, respectively.

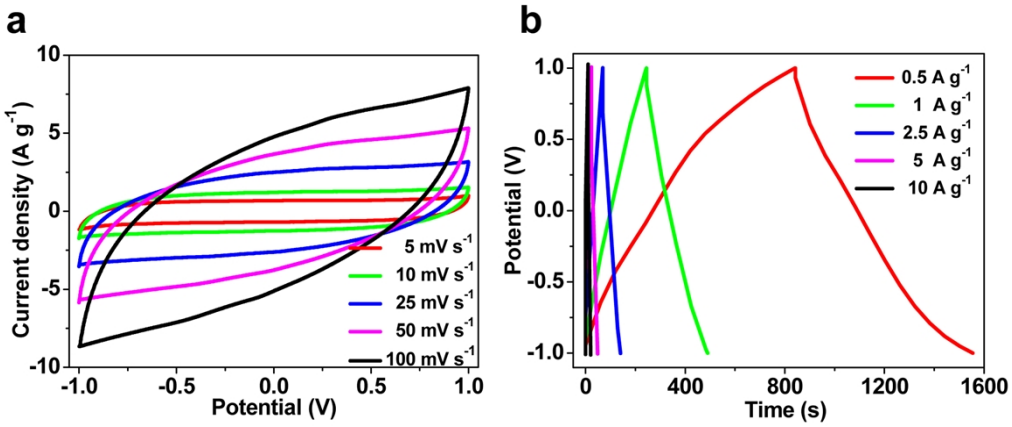

Fig. S11 CV (a) and galvanostatic charge/discharge curves (b) of V_2O_5 aerogel/MWCNTs composite (VMC–30).

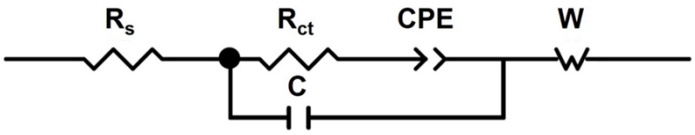

Fig. S12 Electron equivalent circuit to analyze the EIS profiles of raw V_2O_5 powder, synthesized aerogels, V_2O_5 aerogel/MWCNTs composite (VMC–30) and MWCNTs electrodes.

Table S1 The electrolyte resistance (R_e) and charge transfer resistance (R_{ct}) calculated from the EIS profiles of raw V_2O_5 powder, synthesized aerogels, V_2O_5 aerogel/MWCNTs composite (VMC–30) and MWCNTs electrodes.

	V_2O_5	**VA**	**VMA–15**	**VMA–30**	**VMA–60**	**VMA–120**	**MWCNTs**	**VMC–30**
R_e (Ω)	0.52	0.54	0.52	0.52	0.48	0.49	0.48	0.47
R_{ct} (Ω)	49.33	5.87	3.22	2.28	2.27	1.99	1.80	4.82